Catalysis Today 146 (2009) 260–264

Contents lists available at ScienceDirect

Catalysis Today

journal homepage: www.elsevier.com/locate/cattod

Cr-free Fe-based metal oxide catalysts for high temperature water gas shift reaction of fuel processor using LPG

Joon Yeob Lee [a], Dae-Won Lee [b], Kwan-Young Lee [a,*], Yong Wang [c]

[a] Department of Chemical and Biological Engineering, Korea University, 5-1, Anam-dong, Sungbuk-ku, Seoul 136-701, Republic of Korea
[b] Research Institute of Clean Chemical Engineering Systems, Korea University, 1-5, Anam-dong, Sungbuk-ku, Seoul 136-701, Republic of Korea
[c] Pacific Northwest National Laboratory, 902 Battelle Blvd., Richland, WA 99352, USA

ARTICLE INFO

Article history:
Available online 21 March 2009

Keywords:
WGSR
HTS
LPG
Cr-free catalyst
Fuel processor

ABSTRACT

The goal of this study was to identify the most suitable chromium-free iron-based catalysts for the HTS (high temperature shift) reaction of a fuel processor using LPG. Hexavalent chromium (Cr^{6+}) in the commercial HTS catalyst has been regarded as hazardous material. We selected Ni and Co as the substitution for chromium in the Fe-based HTS catalyst and investigated the HTS activities of these Cr-free catalysts at LPG reformate condition. Cr-free Fe-based catalysts which contain Ni, Zn, or Co instead of Cr were prepared by coprecipitation method and the performance of the catalysts in HTS was evaluated under gas mixture conditions (42% H_2, 10% CO, 37% H_2O, 8% CO_2, and 3% CH_4; *R* (reduction factor): about 1.2) similar to the gases from steam reforming of LPG (100% conversion at steam/carbon ratio = 3), which is higher than *R* (under 1) of typically studied LNG reformate condition. Among the prepared Cr-free Fe-based catalysts, the 5 wt%-Co/Fe/20 wt%-Ni and 5 wt%-Zn/Fe/20 wt%-Ni catalysts showed good catalytic activity under this reaction condition simulating LPG reformate gas.

1. Introduction

Fuel cells are one of the most promising new power sources, featuring both cleanliness and versatility [1] and the hydrogen fuel cell, in particular, has engendered extensive research efforts. Among the several types of fuel cells that have been explored, the PEMFC (Polymer Electrolyte Membrane Fuel Cell) appears to be a promising alternative for internal and external combustion engines in transportation or at fixed sites [2–4].

As the gas flow through the PEMFC must contain very little CO to avoid CO-poisoning of Pt electrode [5–7], the fuel processor for industrial applications of PEMFC generally includes a catalytic reformer, water gas shift reaction (WGSR), preferential oxidation (PROX) and/or PSA (pressure swing adsorption) for the removal of CO. Of the available catalytic reforming strategies, steam reforming of methane is the most widely used [5] and LNG is the most effective stock for the hydrogen production method because methane has the highest H/C ratio of any hydrocarbon. However, the infrastructure for hydrogen production should be constructed in areas neighboring a natural gas pipeline due to the large energy investment required for the transport and storage of LNG, which includes the technical difficulties of natural gas liquefaction [8]. On the other hand, LPG is comparatively easy to procure, because facilities for LPG delivery to residential and commercial regions are well established, especially in Korea and Japan [8] and it is regarded as an alternative fuel for LNG for its high availability and low price [8]. Therefore, from the standpoint of making the application more realistic, it would be meaningful to develop an effective LPG fuel processor and integrate it into a fuel cell system. Furthermore, it is meaningful from the viewpoint of diversification of fuel source for hydrogen production, as well.

The WGSR (Eq. (1)) is a main process for hydrogen production from various hydrocarbon sources [9,10].

$$CO + H_2O \rightarrow CO_2 + H_2, \quad \Delta H = -41.1\,kJ/mol \qquad (1)$$

On the basis of thermodynamic and kinetic considerations, WGSR is typically performed in two stages, using a high temperature shift (HTS) and a low temperature shift (LTS) catalyst bed, and it has been established that magnetite (Fe_3O_4) shows the best catalytic activity for HTS [9–11]. A commercial HTS catalyst optimized for the reaction of LNG reformate consists of Fe and Cr species in which chromium(III) oxide (Cr_2O_3) prevents Fe_3O_4 from sintering, while Fe_3O_4 functions as the active component [9]. The composition of fresh commercial Fe-Cr catalyst varies with the manufacturer, but 8 wt%-Cr_2O_3/Fe_3O_4 catalyst is generally used in the commercial HTS processing of LNG reformate [9,11–13]. At present, it has been known that the catalytic activity of Fe-Cr catalyst containing small amounts of Cu is higher than that of the existing Fe-Cr catalyst [12–15].

Prior to initial use of commercial Fe-Cr catalyst, iron(III) oxide (Fe_2O_3), must be converted to magnetite (Fe_3O_4) by a partial

---

[*] Corresponding author. Tel.: +82 2 3290 3299; fax: +82 2 926 6102.
E-mail address: kylee@korea.ac.kr (K.-Y. Lee).

0920-5861/$ – see front matter © 2009 Elsevier B.V. All rights reserved.
doi:10.1016/j.cattod.2009.01.041

reduction through pre-reduction using the reformer product gases, where excess additional steam is introduced to control the proper extent of the reduction [9,11,16,17]. Over-reduction of the catalyst to FeO or Fe causes the loss of the active component (Fe_3O_4) as well as physical damage of the catalyst. In such case, a damaging hot spot can form during the reaction due to exothermic methanation for which metallic iron is known to be a good catalyst [11]. Thus, it is very desirable to avoid over-reduction of the Fe_3O_4 during the pre-reduction as well as the reaction [9,11,18]. It is generally known from industrial experience that, if the reduction factor (R, Eq. (2)) for the reformed gas is maintained at less than 1.2, then over-reduction of Fe_3O_4 is not occurred, while over-reduction consistently occurs when R is greater than 1.6 [9,18].

$$R\,(\text{reduction factor}) = \frac{P_{CO} + P_{H_2}}{P_{H_2O} + P_{CO_2}} \tag{2}$$

Pre-reduction and activity test for WGSR catalyst is generally performed at R under 1 [2,13,15]. In case of LPG reformate, R is about 1.2 without additional steam, which is a little bit higher than R of typically studied reduction gas composition. As the equilibrium of CO conversion is very susceptible to the reactant gas composition and the composition of LPG reformate is different from that of LNG with additional steam, it is very valuable to identify a highly effective catalyst for HTS reaction of LPG reformate.

The fresh and aged commercial HTS Fe-Cr catalysts usually contain levels of about 1 wt% hexavalent chromium (Cr^{6+}), a heavy metal ion very toxic to humans, organisms, or cells, and an undesirable environmental contaminant which is difficult to properly dispose [10]. Especially in Europe, RoHS (Restriction of Hazardous Substances) restricts the use of six hazardous materials including Cr^{6+} in all the electronic/electrical equipments and components [19]. Many researches about Cr-free catalyst for HTS reaction have been performed in the last two decades [20–23]. Recently, Fe-Al-Cu was known as a highly active catalyst for HTS reaction [22,23]. However, the research about Cr-free catalyst for HTS at LPG reformate condition has not been reported yet.

In this study, an Fe-based catalyst, devoid of chromium, is suggested for the HTS step of fuel processing using LPG by testing the HTS activities of a series of prepared Cr-free Fe-based catalysts under LPG reformate conditions. Characterization of catalysts was performed using ICP, BET, and XRD. Ni, Zn, and Co have been selected as the substitution for Cr in Fe-based catalysts since they showed good catalytic activity in syn-gas (CO, H_2) related reactions and the WGSR, respectively [20,21,24–27], as well as the thermal stability of Fe-Co metal particles was reported to be improved with increasing Co content [28]. These activities were then compared with well-known LNG-reformate HTS catalysts under the same conditions.

2. Experimental

2.1. Preparation and characterization of the catalysts

Fe/Cr/Cu catalyst obtained kindly from Johnson Matthey Co. was used as the commercial LNG-reformate optimized HTS catalyst in this study. Fe-based metal oxide catalysts were prepared by a coprecipitation method similarly to Rhodes et al. [12,13]. All metal precursors (purchased from Aldrich) were in nitrate hydrate form, and sodium carbonate and sodium hydroxide (Aldrich) were used as the precipitant. Initially, metal nitrate hydrate precursors were dissolved together in deionized water with appropriate ratios to yield the desired metal weight ratio in the product. Sodium carbonate was subsequently added to produce pH 2.75, the brown solution was heated at 70 °C for 1 h, and sodium hydroxide was added to pH 7.5, forming a precipitate. After filtering, the precipitate was washed repeatedly with sufficient deionized water, dried at 110 °C for 24 h, and calcined at 500 °C for 5 h. The notations of the prepared catalysts are shown in Table 1.

Table 1
The notations of the prepared catalysts.

Notation	Description of the prepared catalyst	
	Desired weight ratio	Weight ratio from ICP analysis
Fe100	100 wt%-Fe	N.M.[a]
FeCo20	Fe/20 wt%-Co	N.M.[a]
FeNi8	Fe/8 wt%-Ni	N.M.[a]
FeNi20	Fe/20 wt%-Ni	Fe/23.3 wt%-Ni
Cu2FeCr8	2 wt%-Cu/Fe/8 wt%-Cr	N.M.[a]
Cu5FeCr10	5 wt%-Cu/Fe/10 wt%-Cr	5.2 wt%-Cu/Fe/10.3 wt%-Cr
Zn5FeNi20	5 wt%-Zn/Fe/20 wt%-Ni	5.4 wt%-Zn/Fe/22.3 wt%-Ni
Co5FeNi20	5 wt%-Co/Fe/20 wt%-Ni	5.1 wt%-Co/Fe/23.1 wt%-Ni
Zn5FeCo20	5 wt%-Zn/Fe/20 wt%-Co	N.M.[a]
Ni5FeCo20	5 wt%-Ni/Fe/20 wt%-Co	N.M.[a]

[a] Not measured.

The metal contents of the catalysts were determined by inductively coupled plasma atomic emission spectrophotometer (ICP/AES, 138 Ultrace, Jobin Yvon), powder X-ray diffraction patterns obtained using a D/max-2500 (Rigaku) with Cu Kα (λ = 1.54056 Å) radiation generated at 40 kV and 150 mA, and the BET surface areas of the products measured with a ASAP 2010 (Micrometrics).

2.2. HTS activity measurement

In consideration of the equilibrium composition of LPG steam reformate after the LPG conversion of 100% at steam/carbon ratio = 3 (further information about the LPG used is confidential), a gas composition of CH_4, CO, CO_2, H_2, and H_2O at 3, 10, 8, 42, and 37 vol%, respectively, was used as the HTS reactant composition. Considering the temperature at the steam reformer outlet, isothermal tests for the HTS reaction were performed at 375 and 400 °C with steam fed to the reactor by a syringe pump and other gases individually introduced via a mass flow controller (5850E, Brooks). A catalyst (150–250 μm) was packed over a quartz wool bed located in the middle of a stainless steel tube reactor (ID = 12.5 mm), and water was separated from the outlet gases using a cold-trap at 0 °C, after which the gases were analyzed by on-line gas chromatography (Acme 6000 M, Young Lin) equipped with a Porapak Q (6 ft × 1/8 in. SS, Supelco) column and TCD detector.

3. Results and discussion

3.1. Activities of LNG optimized HTS catalysts under LPG reformate conditions

An Fe/Cr catalyst to which 2 wt% Cu is added yields a Fe/Cr/Cu catalyst that is well known as a good catalyst for the HTS reaction of LNG reformate [12,13,15]. A commercial HTS catalyst (Fe/Cr/Cu, Johnson Matthey) and two prepared catalysts (Cu2FeCr8 and Cu5FeCr10) were examined here to evaluate the applicability of the catalysts in the HTS reaction for LPG reformate. The isothermal experiments were performed under reactant composition described above at 400 °C and a gas hourly space velocity (GHSV) of 25,000 ml/g_{cat} h for about 10 h and the CO conversion was assessed (Fig. 1). Under these conditions the equilibrium CO conversion was estimated to be about 77.2% [11,29].

The average CO conversions of the commercial and the prepared Cu5FeCr10 and Cu2FeCr8 catalysts were about 45.1%,

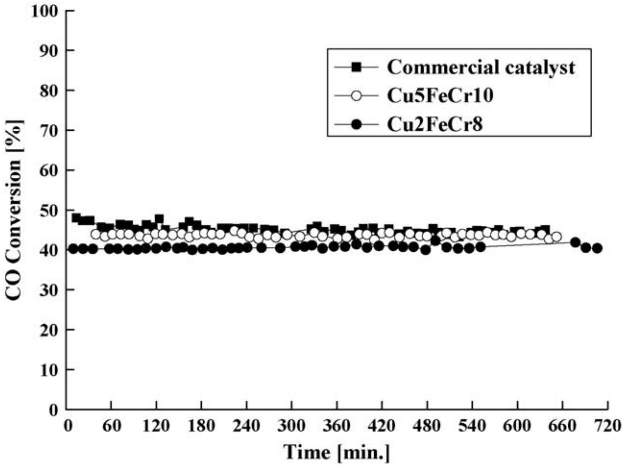

Fig. 1. CO conversions of prepared catalysts (Cu2FeCr8 and Cu5FeCr10) and a commercial catalyst (Johnson Matthey) at 400 °C as a function of time.

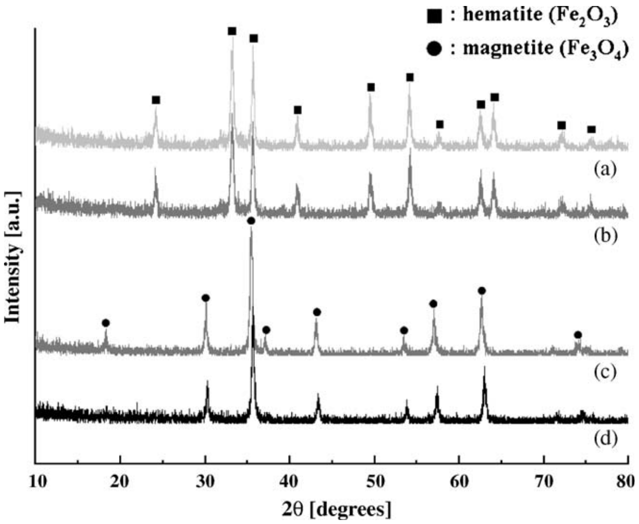

Fig. 2. XRD patterns of prepared catalysts and after reaction at 400 °C for 3 h, respectively: (a) Cu2FeCr8 (fresh); (b) Cu5FeCr10 (fresh); (c) Cu2FeCr8 (after reaction); (d) Cu5FeCr10 (after reaction).

43.7% and 40.6%, respectively, showing similarity (Fig. 1). From X-ray diffraction patterns of the fresh Cu2FeCr8 and Cu5FeCr10 catalysts, only hematite species (Fe_2O_3, JCPDS 33-0664) was detected (Fig. 2). It means that Cu and Cr were in solution with iron oxides, rather than in separate regions of CuO and Cr_2O_3, which was similar to results reported by Edwards et al. [15]. On the other hand, the magnetite (Fe_3O_4, JCPDS 19-0629), which has been known as an active species for HTS by other research groups [9–11], was observed to dominate in aged catalysts after reaction at 400 °C for 3 h.

The catalytic activities of Cu2FeCr8 and Cu5FeCr10 were stable for 10 h (Fig. 1). Therefore, it is expected that a separate pre-reduction step for Cr-containing Fe-based catalysts is not required, especially in our reaction condition simulating LPG reformate gas. Fe/Cr/Cu has been known as the best catalyst for the HTS reaction of LNG reformate [9–13,30], but the CO conversions of these catalysts were lower than 50% in the present LPG-reformate HTS conditions.

3.2. BET results and catalytic activities of two component Fe-based catalysts

Various Cr-free Fe-based catalysts were prepared by the coprecipitation method and the surface area, pore volume and pore diameter were evaluated (Table 2). The prepared iron oxide catalyst had a BET surface area of 21.1 m^2/g and, notably, the BET surface area increased to 30–65 m^2/g as other metals were introduced to the catalyst.

Single and two component Fe-based catalysts (Fe100, FeNi8, FeNi20 and FeCo20) were examined in the HTS reaction at 400 °C for 3 h. The results of CO conversions of the catalysts showed that the addition of Ni and Co increased the catalytic activity of the Fe (Fig. 3). Average CO conversions of Fe100, FeCo20, FeNi8 and FeNi20 catalysts were about 26.3%, 39.2%, 50.6% and 67.6%, respectively. The CO conversion of the FeCo20 catalyst was lower than the 45.1% of commercial catalyst under these conditions, but the CO conversion by the FeNi8 and FeNi20 catalysts at 400 °C were higher than the commercial catalyst, with the CO conversion by the FeNi20 catalyst over 65%.

3.3. Catalytic activities of three component Fe-based catalysts and X-ray diffraction results

Isothermal catalytic activity examinations of three component Fe-based catalysts for the HTS reaction were performed at 375 and 400 °C for 3 h. Using the reaction composition described previously, the equilibrium CO conversions were calculated to be 81.6% at 375 and 77.2% at 400 °C, respectively (Fig. 4) [11,29]. These results showed that CO conversions of the Zn5FeNi20 and Co5FeNi20 catalysts were both over 65% at 375 and 400 °C, while CO conversions of the Zn5FeCo20 and Ni5FeCo20 catalysts were under 55%, and the former two catalysts showed enhanced CO conversions compared to commercialized LNG-reformate opti-

Table 2
The results (surface area, pore volume and pore diameter) of BET analysis and inverse spinel crystallite size from XRD data of various catalysts prepared by coprecipitation method.

Catalyst	BET analysis			Inverse spinel crystallite size[a] [nm]
	Surface area [m^2/g]	Pore volume [cm^3/g]	Pore diameter [nm]	
Fe100	21.1	0.099	19	40.0
FeCo20	31.7	0.191	24	N.M.[b]
FeNi8	32.2	0.201	25	N.M.[b]
FeNi20	44.3	0.169	15	29.9
Cu2FeCr8	29.2	0.238	33	22.8
Cu5FeCr10	30.2	0.192	25	23.7
Zn5FeNi20	64.8	0.158	10	21.4
Co5FeNi20	51.5	0.138	11	23.4
Zn5FeCo20	48.7	0.155	13	N.M.[b]
Ni5FeCo20	52.1	0.186	14	N.M.[b]

[a] Crystallite size after reaction at 400 °C for 3 h.
[b] Not measured.

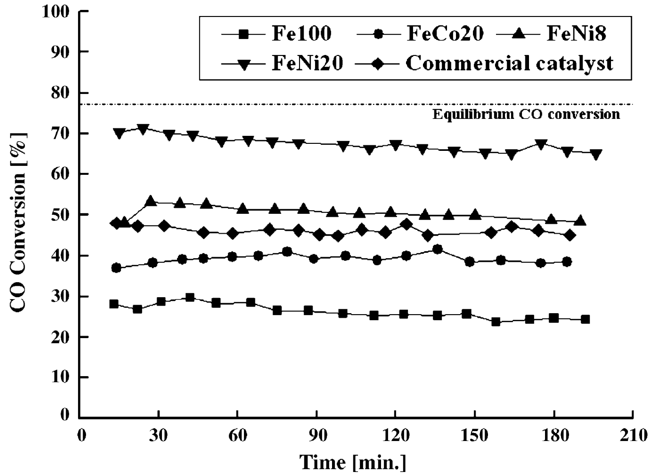

Fig. 3. CO conversions of Fe100, FeCo20, FeNi8, FeNi20 and commercial catalyst as a function of time and equilibrium CO conversion at 400 °C.

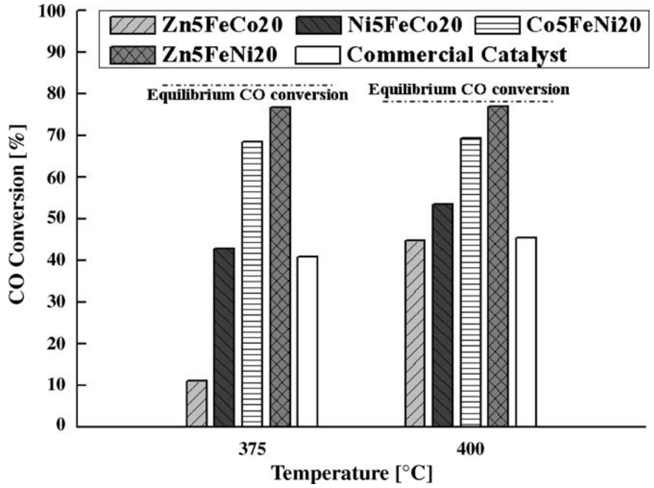

Fig. 4. CO conversions of three component catalysts at 375 and 400 °C.

mized catalysts and the two component Fe-based catalysts (Figs. 1 and 3). In the case of Zn5FeNi20, CO conversions were 76.6% and 77% at 375 and 400 °C, respectively, close to the equilibrium CO conversion. From the performances of the Zn5FeNi20 and Zn5FeCo20 catalysts, it was concluded that the addition of 5 wt% Zn generally improved the catalytic activities of Fe/Ni and Fe/Co catalysts. CO conversion by the Co5FeNi20 catalyst was higher than the Ni5FeCo20 catalyst, in spite of the fact they were the same metals simply in different proportions. It thus appeared that the specific metal additives and their proportions were important factors in screening for useful three component Fe-based HTS catalysts.

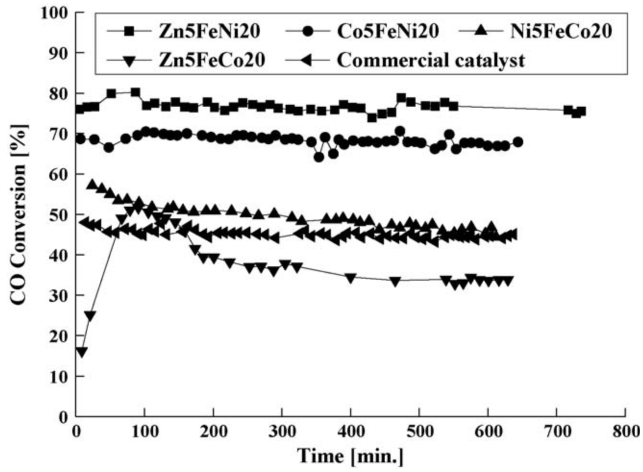

Fig. 5. CO conversions of commercial and prepared three component catalysts at 400 °C as a function of time.

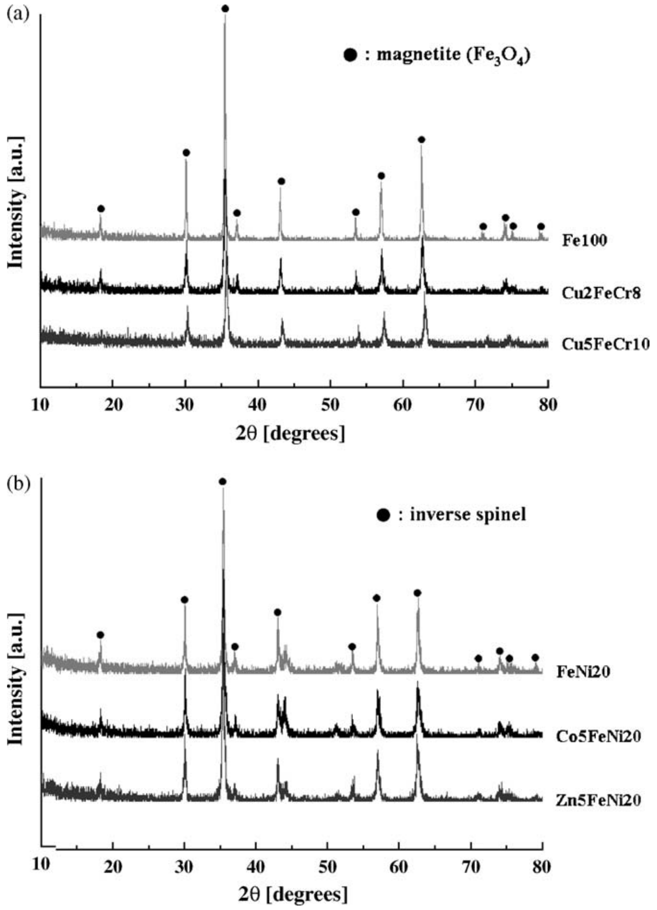

Fig. 6. XRD patterns of prepared catalysts after reaction at 400 °C for 3 h: (a) Fe100 and Cr-containing catalysts (Cu2FeCr8 and Cu5FeCr10); (b) Ni-containing Cr-free Fe-based catalysts (FeNi20, Zn5FeNi20 and Co5FeNi20).

The isothermal tests on various three component Fe-based catalysts performed for longer times (∼10 h) at 400 °C, and CO conversion was evaluated as a function of time (Fig. 5). CO conversion by the Ni5FeCo20 catalyst was slightly higher than the commercial catalyst at 400 °C. The Zn5FeCo20 catalyst initially showed better catalytic activity than the commercial catalyst, but after 80 min CO conversion gradually decreased and finally stabilized at 34% after 6 h. The Zn5FeNi20 and Co5FeNi20 catalysts showed CO conversions higher than any other catalysts and, moreover, their catalytic activities were comparatively stable for about 10 h.

Powder X-ray diffraction patterns of Fe-based catalysts revealed the absence of crystalline phases related to Cu, Cr, Zn, Co, and Ni in all cases with exception of the peaks at 44° and 52° in Ni-containing catalysts (Fig. 6), which can be attributed to the formation of a homogeneous solid solution or amorphous phase [15,17,31]. The inverse spinel type crystalline was observed to dominate in all catalysts. The X-ray diffraction peaks of Cu2FeCr8 and Cu5FeCr10 catalysts were broader than the Fe100, indicating that the magnetite crystallite sizes of these catalysts were smaller than the Fe100 catalyst. The XRD peaks of Zn5FeNi20 and Co5FeNi20 catalysts were broader than the FeNi20 in case of Ni-containing Cr-free Fe-based catalysts, which exhibits the similar phenomenon as Cr-containing catalysts. The inverse spinel crystalline sizes in all catalysts were calculated using the Scherrer equation applied to the [311] ($2\theta = 35.422^\circ$ and 35.684°) diffraction peaks [32] (Table 2). The dominance of the inverse spinel crystalline phase and its small crystallite size were assumed here to be two causes of their high activities (Figs. 4 and 5).

4. Conclusions

Cr-free Fe-based metal oxide catalysts constituted with two or three metal components were prepared by a coprecipitation method. The BET surface area of prepared catalysts increased with the addition of other metals to the Fe. Among the prepared catalysts, Zn5FeNi20 and Co5FeNi20 catalysts showed good catalytic activity (around 65–75% CO conversion at 400 °C) in the HTS condition of LPG reformate. Furthermore, the CO conversions on these catalysts were higher than the CO conversion on commercial catalyst optimized for HTS reaction of LNG reformate and, particularly, the Zn5FeNi20 catalyst exhibited CO conversion quite close to the equilibrium conversion. In addition, the catalytic activities of the Zn5FeNi20 and Co5FeNi20 catalysts were comparatively stable for 10 h under these conditions.

Acknowledgement

This work was supported by the Korea Research Foundation Grant (KRF-2008-013-D00025).

References

[1] B. Silberova, H.J. Venvik, J.C. Walmsley, A. Holmen, Catal. Today 100 (2005) 457–462.
[2] G. Jacobs, E. Chenu, P.M. Patterson, L. Williams, D. Sparks, G. Thomas, B.H. Davis, Appl. Catal. A 258 (2004) 203–214.
[3] G. Avgouropoulos, T. Ioannides, Appl. Catal. A 244 (2003) 155–167.
[4] T. Tabakova, F. Boccuzzi, M. Manzoli, J.W. Sobczak, V. Idakiev, D. Andreeva, Appl. Catal. A 298 (2006) 127–143.
[5] F.A. de Bruijn, B. Rietveld, R.W. van den Brink, in: G. Centi, A. van Santen (Eds.), Catalysis for Renewables, Wiley-VCH, Weinheim, 2007, pp. 299–336.
[6] R.A. Dagle, Y. Wang, G-.G. Xia, J.J. Strohm, J. Holladay, D.R. Palo, Appl. Catal. A 326 (2007) 213–218.
[7] J-.H. Wee, K-.Y. Lee, J. Power Sources 157 (2006) 128–135.
[8] S. Takenaka, K. Kawashima, H. Matsune, M. Kishida, Appl. Catal. A 321 (2007) 165–174.
[9] C. Rhodes, G.J. Hutchings, A.M. Ward, Catal. Today 23 (1995) 43–58.
[10] K. Kochloefl, in: G. Ertl, H. Knözinger, J. Weitkamp (Eds.), Handbook of Heterogeneous Catalysis, vol. 4, Wiley-VCH, Weinheim, 1997, pp. 1831–1843.
[11] L. Lloyd, D.E. Ridler, M.V. Twigg, in: M.V. Twigg (Ed.), Catalyst Handbook, 2nd ed., Wolfe Publishing Ltd., London, 1989, pp. 283–339.
[12] C. Rhodes, G.J. Hutchings, Phys. Chem. Chem. Phys. 5 (2003) 2719–2723.
[13] C. Rhodes, B.P. Williams, F. King, G.J. Hutchings, Catal. Commun. 3 (2002) 381–384.
[14] A. Andreev, V. Idakiev, D. Mihajlova, D. Shopov, Appl. Catal. 22 (1986) 385–387.
[15] M.A. Edwards, D.M. Whittle, C. Rhodes, A.M. Ward, D. Rohan, M.D. Shannon, G.J. Hutchings, C.J. Kiely, Phys. Chem. Chem. Phys. 4 (2002) 3902–3908.
[16] A.L.C. Pereira, G.J.P. Berrocal, S.G. Marchetti, A. Albornoz, A.O. de Souza, M.C. Rangel, J. Mol. Catal. A 281 (2008) 66–72.
[17] I.L. Júnior, J-.M.M. Millet, M. Aouine, M.C. Rangel, Appl. Catal. A 283 (2005) 91–98.
[18] W.J. Lywood and M.V. Twigg, Eur. Patent No. 0361648 (1990).
[19] Official Journal of the European Union, 46 (2003) 19–37.
[20] F.M. Gottschalk, G.J. Hutchings, Appl. Catal. 51 (1989) 127–139.
[21] F.M. Gottschalk, R.G. Copperthwaite, M.V.D. Riet, G.J. Hutchings, Appl. Catal. 38 (1988) 103–108.
[22] G.C. Araújo, M.C. Rangel, Catal. Today 62 (2000) 201–207.
[23] S. Natesakhawat, X. Wang, L. Zhang, U.S. Ozkan, J. Mol. Catal. A 260 (2006) 82–94.
[24] St.G. Christoskova, M. Stoyanova, M. Georgieva, Appl. Catal. A 208 (2001) 235–242.
[25] G. Grubert, S. Kolf, M. Baerns, I. Vauthey, D. Farrusseng, A.C. Veen, C. Mirodatos, E.R. Stobbe, P.D. Cobden, Appl. Catal. A 306 (2006) 17–21.
[26] J.G. Seo, M.H. Youn, H-.I. Lee, J.J. Kim, E. Yang, J.S. Chung, P. Kim, I.K. Song, Chem. Eng. J. 141 (2008) 298–304.
[27] D.H. Kim, J.W. Ryu, E.H. Choi, G.T. Gong, H. Lee, B.G. Lee, D.J. Moon, Catal. Today 136 (2008) 266–272.
[28] H. Tetsukawa, M. Inoue, H. Kondo, J. Magn. Magn. Mater. 269 (2004) 423–428.
[29] J.M. Smith, H.C.V. Ness, M.M. Abbott, Introduction to Chemical Engineering Thermodynamics, 6th ed., McGraw-Hill, New York, 2001, pp. 486–488.
[30] C.N. Satterfield, Heterogeneous Catalysis in Industrial Practice, 2nd ed., McGraw-Hill, New York, 1991, pp. 442–444.
[31] P.S. Querino, J.R.C. Bispo, M.C. Rangel, Catal. Today 107–108 (2005) 920–925.
[32] C. Suryanarayana, M.G. Norton, X-Ray Diffraction: A Practical Approach, Plenum Press, New York, 1998, pp. 212–213.